Favorable power conversion efficiencies in organic solar cell bulk-heterojunctions

Juliane M. Scholtz

Department of Physics, Cornell University, Ithaca, NY 14853

Mentored by Dr. Selman Hershfield

Department of Physics, University of Florida, Gainesville, FL 32611

Abstract

Organic solar cells presently demonstrate much smaller power conversion efficiencies than their inorganic counterparts. Research suggests a direct link between power conversion efficiency and the morphology of the organic solar cell's bulk-heterojunction. This paper describes efforts to find an optimal organic solar cell bulk-heterojunction morphology using simulations developed in MATLAB. Three different computer-generated morphologies were considered. The first sample type had the percentages of p-type and n-type materials uniform throughout the sample. The second used a linearly varying percentage pair. The third sample type consisted of a large middle region with its percentage pair, capped at the ends by regions subject to a second p-n ratio. Favorable power densities were found in the samples with 60% p-type/40% n-type throughout, as well as in the capped samples with percentages 50%-50%--60%-40%--50%-50%. In contrast, the second sample type displayed poor net power densities.

I. INTRODUCTION

Although solar cells were first developed in the 1950s,[1] various limitations still impede their wide-spread use. Despite their high efficiencies, inorganic solar cells have proven very costly for environmentally-conscious consumers.[2] An alternate solar technology, organic bulk-heterojunction photovoltaics, has been the subject of extensive scientific research.[3] Organic solar cells (OSCs) possess many advantages over their inorganic counterparts, including flexibility,[1] low manufacturing and purchase costs,[3,4] and short energy payback times.[4] The greatest challenge to the wide-scale marketability of organic solar cells remains their low Power Conversion Efficiency (PCE),[4,5] the ratio of output power to input power**.** In 2016, this value was approximately 11%.[6] Organic photovoltaics' capability to compete with traditional silicon solar cells, whose efficiencies range as high as 26%,[6] is greatly limited at this time. Further research is therefore needed to make organic solar cells appealing to consumers.

All solar cells contain two kinds of materials: a donor (p-type) and an acceptor (n-type) material, which lose and gain electrons, respectively.[5] These materials can be arranged in the form of the planar heterojunction (Fig.1a), or in that of the bulk-heterojunction (Fig. 1b).

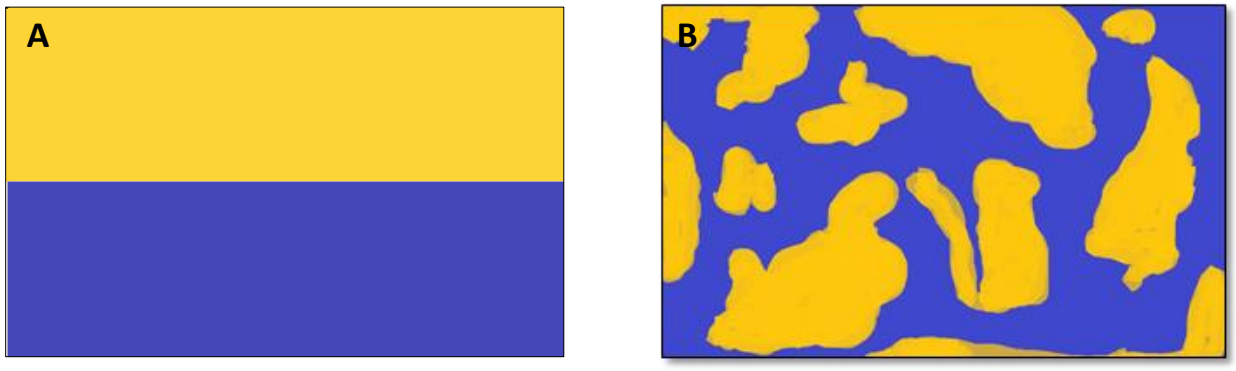

Figure 1. a). A planar heterojunction (PHJ), with donor (yellow) and acceptor (purple) materials laid next to each other in layers. **b).** A bulk-heterojunction (BHJ), with donor and acceptor materials scattered throughout.

The bulk-heterojunction provides a greater power conversion efficiency than the planar heterojunction due to its increased interface area between the donor and acceptor materials.[5] Light striking the organic solar cell produces *excitons*, particles consisting of an excited electron and an electron "hole".[7] These excitons *dissociate*, or break into their original components, only at such donor-acceptor interfaces.[4] This separation process permits free charge carriers (holes and electrons) to move through the bulk-heterojunction to the proper electrodes, producing a usable electrical current.[5,8] A high interface surface area should therefore provide high power output. In certain BHJ compositions (*morphologies*), however, dissociated electrons and holes can encounter carriers of the opposite type and join themselves to these entities, reducing the amount of mobile carriers.[8] This process of *recombination* therefore reduces the electric current and power generated by the organic solar cell.[8]

The precise donor-acceptor arrangement which will maximize power conversion efficiency and interface surface area remains unknown[4] and forms the subject of this paper. Section II describes the electrical models used to perform OSC simulations in MATLAB R2014b, while Sec. III notes analytic and physical concerns addressed in the developed scripts. Sec. IV discusses power outputs of several generated OSC samples, and is followed by closing remarks in Sec. V.

II. ELECTRICAL MODELS OF ORGANIC SOLAR CELLS [9]

Modelling current flows and net power requires knowledge of the voltage and current at many locations inside the three-dimensional OSC. I will illustrate an iterative method in one dimension which was later incorporated into the three-dimensional MATLAB simulations. This

iterative process is well-suited for the analysis of large solar cell samples, such as those of dimension 40x40x20 units.

Consider a one-dimensional string of N resistors in series, with N+1 nodes (Figure 1). Electric potentials V_1 and V_{N+1}, as well as all conductances $G_1 \ldots G_N$,

$$G_i = 1/R_i \qquad 1 \leq i \leq \mathrm{N}, \qquad (1)$$

are known.

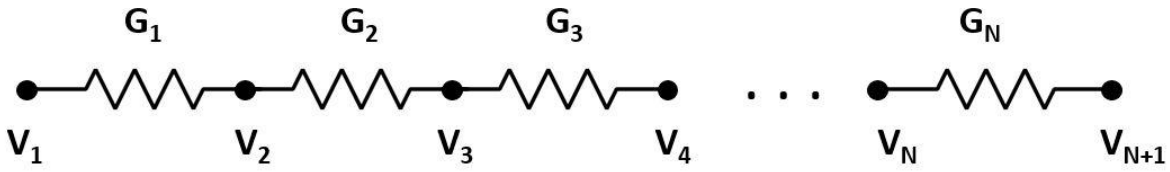

Figure 2. String of N resistors.

To determine the interior potentials, two fundamental rules of circuits are used.[10] Beginning with Ohm's Law, the current through any resistor i, $1 \leq i \leq \mathrm{N}$, is

$$I_i = G_i (V_{i+1} - V_i) . \qquad (2)$$

By Kirchhoff's Junction Rule, the net current flowing through any node j, $2 \leq j \leq \mathrm{N}$, is

$$\Sigma I_j = 0 . \qquad (3)$$

Substituting (2) into (3) gives

$$G_{j-1} (V_{j-1} - V_j) + G_j (V_{j+1} - V_j) = 0. \qquad (4)$$

Expand and rearrange terms:

$$(G_{j-1} + G_j) V_j = G_{j-1} V_{j-1} + G_j V_{j+1} \quad . \qquad (5)$$

Thus, the electrical potential at any interior node j, $2 \leq j \leq \mathrm{N}$, is

$$V_j = (G_{j-1} V_{j-1} + G_j V_{j+1}) / (G_{j-1} + G_j) \quad , \qquad (6)$$

and the current through any resistor i, $1 \leq i \leq \mathrm{N}$, is then calculated via (2).

As only the electric potentials V_1 and V_{N+1} are initially known, Equation (6) must be used repeatedly to determine the remaining potentials. This amounts to a system of N-1 equations with N-1 unknowns. The success of this iterative process (*relaxation method*) [11] is determined by the convergence of the currents I_i, $1 \leq i \leq$ N. After a sufficient number of iterations, all I_i will be equal and thus satisfy Ohm's Law over the entire string ($I_i = I = G_{tot}(V_{N+1} - V_1)$).[12] This one-dimensional example may be applied to the three-dimensional OSC, where six terms (four for neighboring resistors in the x-y plane, two for those in the +z and –z directions) form the left-hand side of Eqn. (4). Boundaries between donor-donor and acceptor-acceptor materials in the generated bulk-heterojunctions[13] were modelled as resistors, while donor-acceptor interfaces were treated as diodes, each with their respective J-V characteristics. The entire BHJ was analyzed as a three-dimensional matrix of donor and acceptor materials, adjacent to a cathode and an anode (Figure 3). The resulting net power in the z- (vertical) direction was measured in at least ten samples of each morphology type generated.[14]

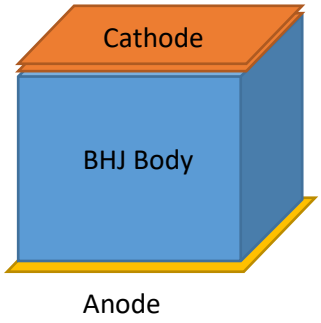

Figure 3. Structure of the simulated OSCs.

III. PHYSICAL AND ANALYTIC CONSIDERATIONS

OSC sample size, the need for equivalent I_i and simulation run time were important issues in the course of this project. Larger samples, such as size 40x40x40 units, and tall, non-cubic

samples, such as size 10x10x40 units, did not show successful convergence of the I_i within a reasonable run time for this project. With the chosen sample of size 20x20x20 units, a concentrated search for the proper N_{iter} was necessary. Figure 4a shows that the conservation of current is violated (I_i do not converge) with a too-small N_{iter} value. In contrast, 8000 iterations provided the necessary convergence, as shown in Figure 4b. Here, the vertical current *jznet* is independent of z-coordinates, indicating a conservation of current. The value N_{iter} = 8000 was used as the default in all future simulations, and the currents periodically examined to ensure convergence.

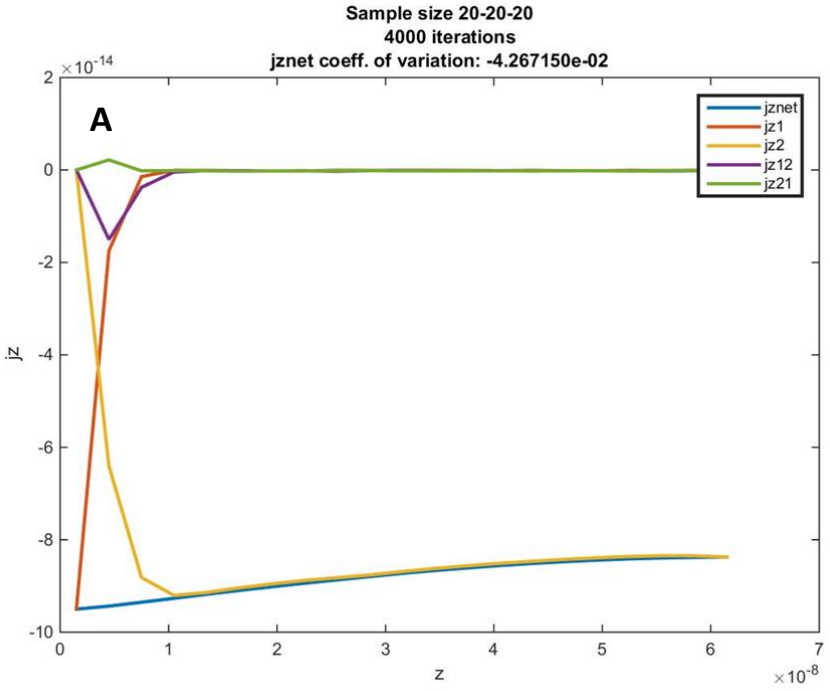

Figure 4 a). Plot of various currents vs. vertical location in the BHJ. The blue curve shows the net current in the z (vertical) direction. Its non-horizontal nature indicates lack of I_i convergence when N_{iter} = 4000.

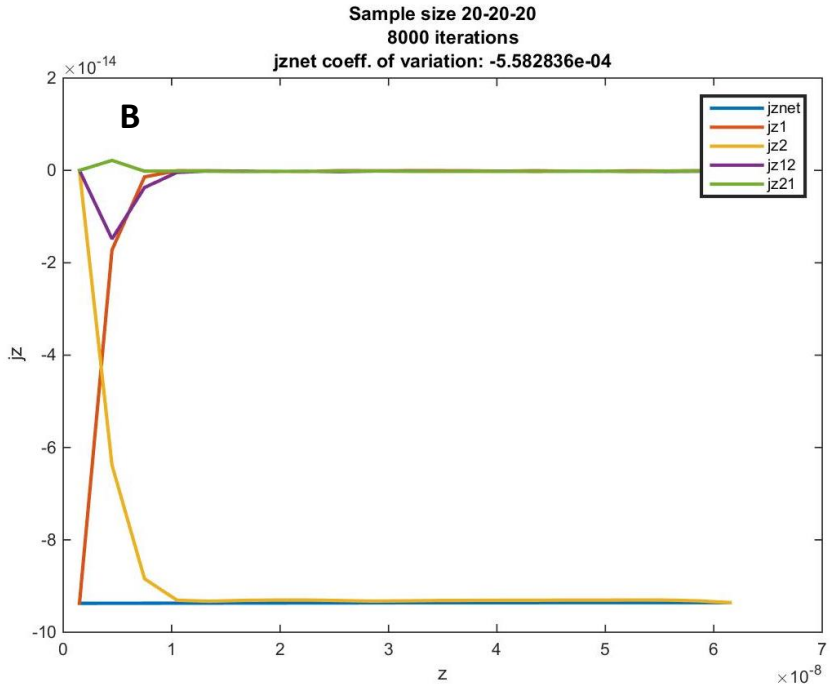

Figure 4 b). Vertical current is conserved, shown by the horizontal blue line. Doubling N_{iter} decreased the coefficient of variation of jznet by 98.7%.

Although the cubic 20x20x20 sample was chosen for all testing, the simulations indicate that a short, wide sample will provide more uniform power density results for a given number of BHJ's generated. Having generated ten random samples for each of five different sizes, the scripts created histograms to analyze the variation in power density results between runs performed for a specific sample size (Figures 5a-e). The standard deviation decreased from 2.962 x 10^{-18} Watts/Area in the 20x20x20 samples to 1.261 x 10^{-18} Watts/Area in the 60x60x20 bulk-heterojunctions. The power densities in the 20x20x20 samples fall over a range of 0.095 x 10^{-16} W/Area, while this value, at 0.042 x 10^{-16} W/Area, is somewhat smaller for the 60x60x20 sample. This slight improvement did not justify the use of the 60x60x20 sample over the smaller 20x20x20 piece, as the former required exceedingly long run times. Instead, 20x20x20 was the set of dimensions chosen for use throughout this project.

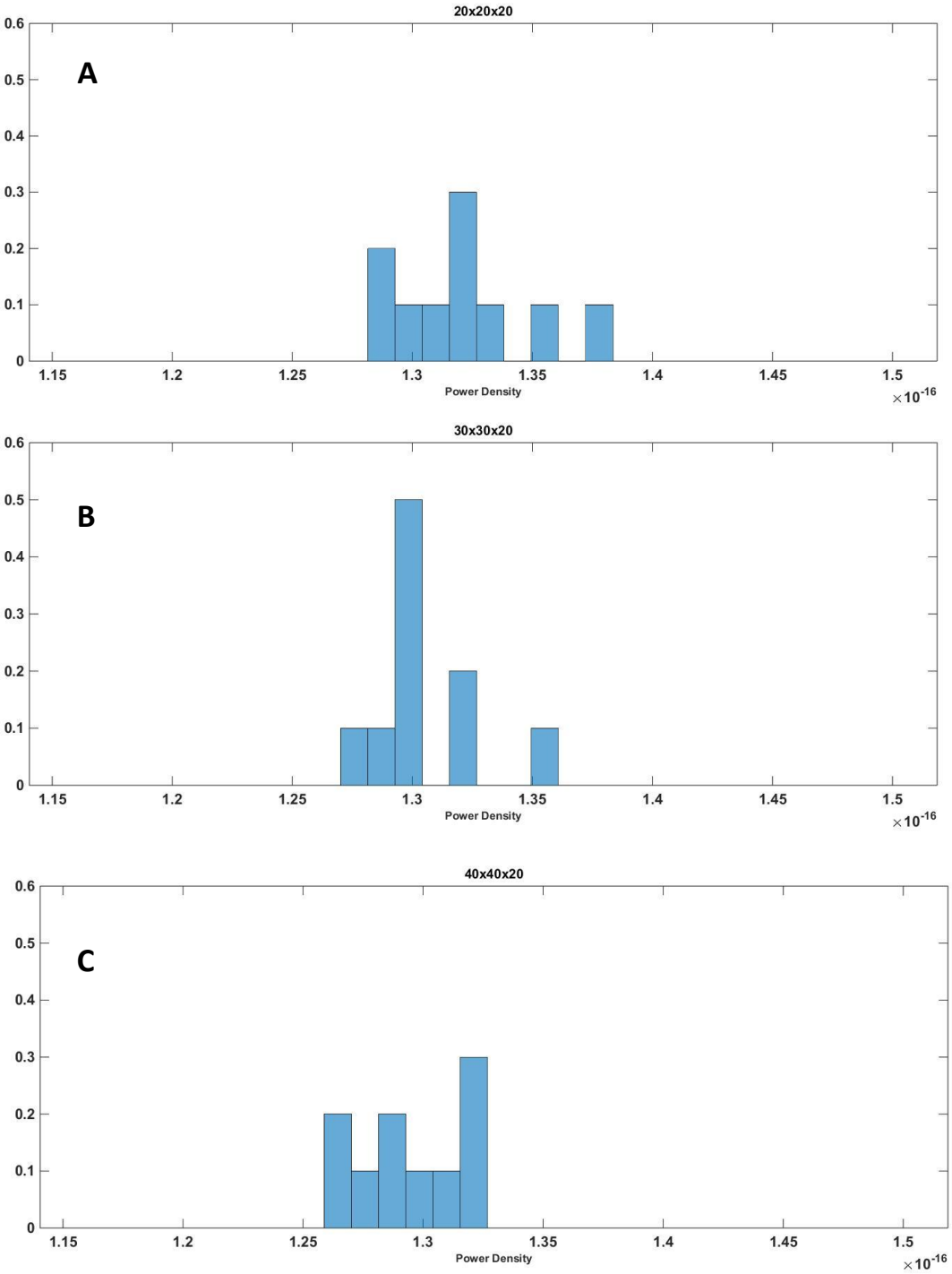

Figure 5. Histograms of net power densities for various BHJ sample sizes. **a).** 20x20x20 sample; **b).** 30x30x20 sample**; c).** 40x40x20 sample.

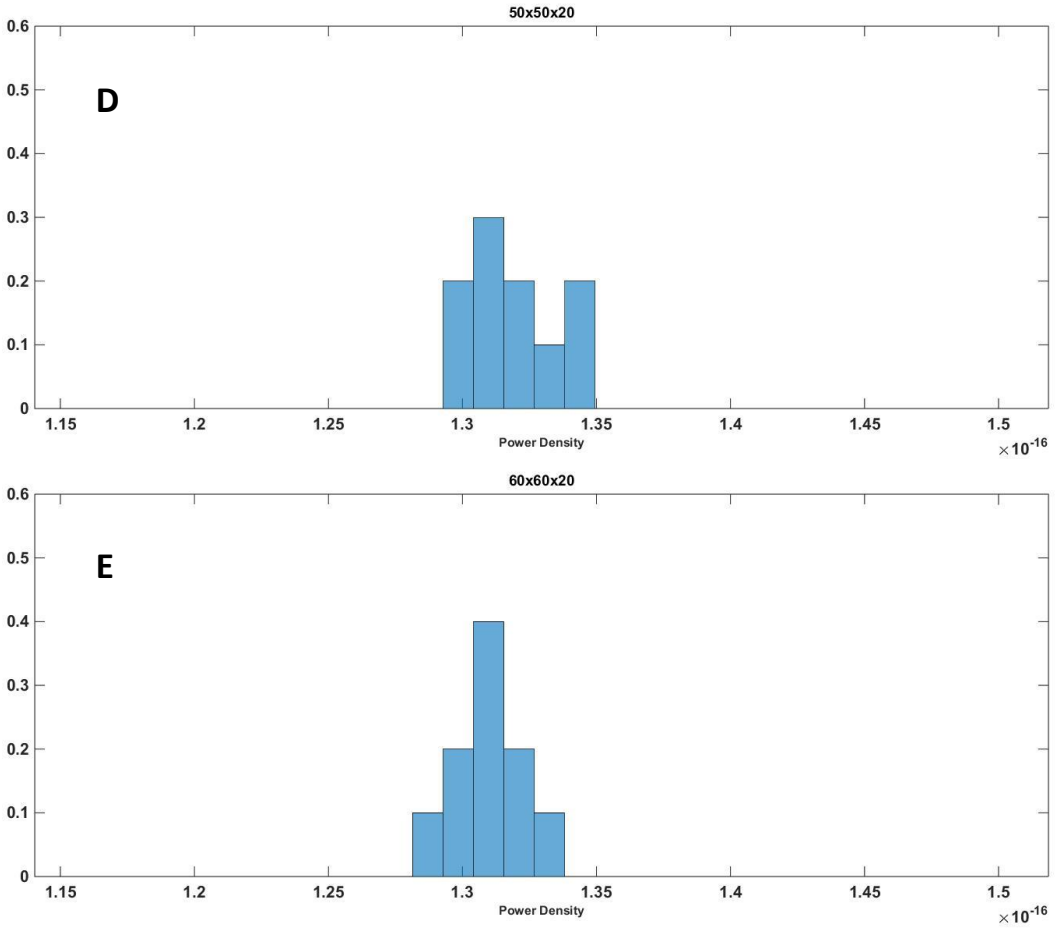

Figure 5. Histograms of net power densities for various BHJ sample sizes. **d).** 50x50x20 sample; **e).** 60x60x20 sample.

IV. GENERATED SAMPLES

A. Uniform Weighted-Sum Sample

In this set of simulations, the p-type and n-type materials were assigned specific probabilities of being found in any layer parallel to the x-y plane of the OSC. A foundational code portion then generated BHJs subject to these probabilities. The power density results for many different probability pairs are shown in Figure 6. The sample with p-n probabilities of 60% and 40%, respectively, provides the greatest mean power density over ten runs. This is likely due to the conductivity relationship between the two materials: the p conductivity measured twice that of the n conductivity.

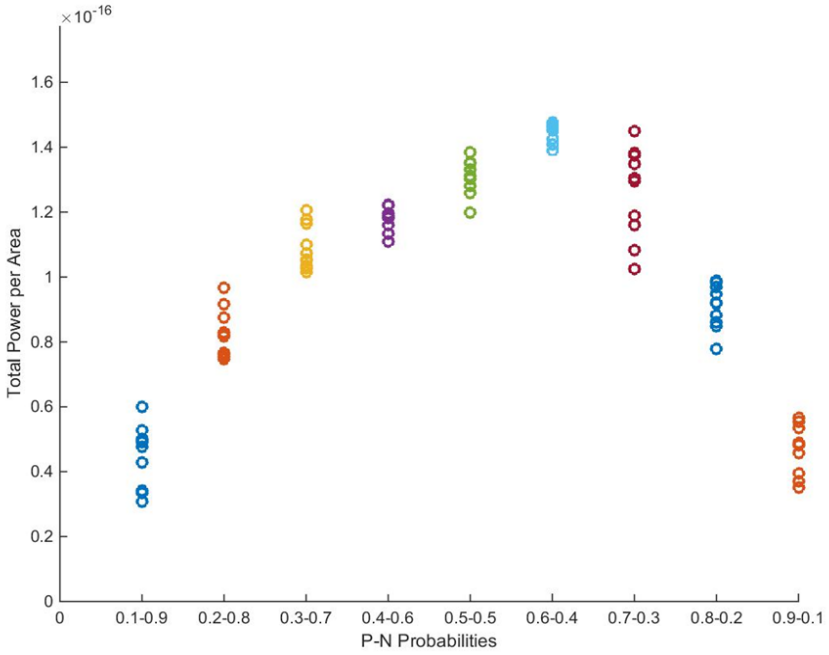

Figure 6. Power density as a function of donor-acceptor probability pair. Each probability pair condition was applied ten times, corresponding to the ten plotted circles per horizontal tick mark. Default p- and n-material conductivities were used. The mean power density at the 60%-40% mark is 1.45 x 10^{-16} W/Area.

This project, with its use of non 50%-50% probability pairs, allows broader analysis of BHJ morphology than that performed by Schlittenhardt,[15] whose work reveals the importance of high interface area in various 50%-50% random OSC samples. The results of this section demonstrate potentially favorable BHJ morphologies using non- 50%-50% samples.

A noteworthy change in power densities occurs when the conductivities of the donor/acceptor materials are altered. The default p-type conductivity (σ_1) was $9.26 \times 10^{-5} (\Omega*m)^{-1}$, while the n-type conductivity (σ_2) satisfied $\sigma_2 = (0.5*\sigma_1) = 4.63 \times 10^{-5} (\Omega*m)^{-1}$. As σ_2 was repeatedly halved, the power density graph developed an apparent saddle point at 30%-70%, with the most favorable samples still located near the 60%-40% mark (Figure 7a-b). Further testing with additional probability pairings (15%-85%, 25%-75%, 35%-65%) is needed to determine the precise significance of the change near the 30%-70% pair.

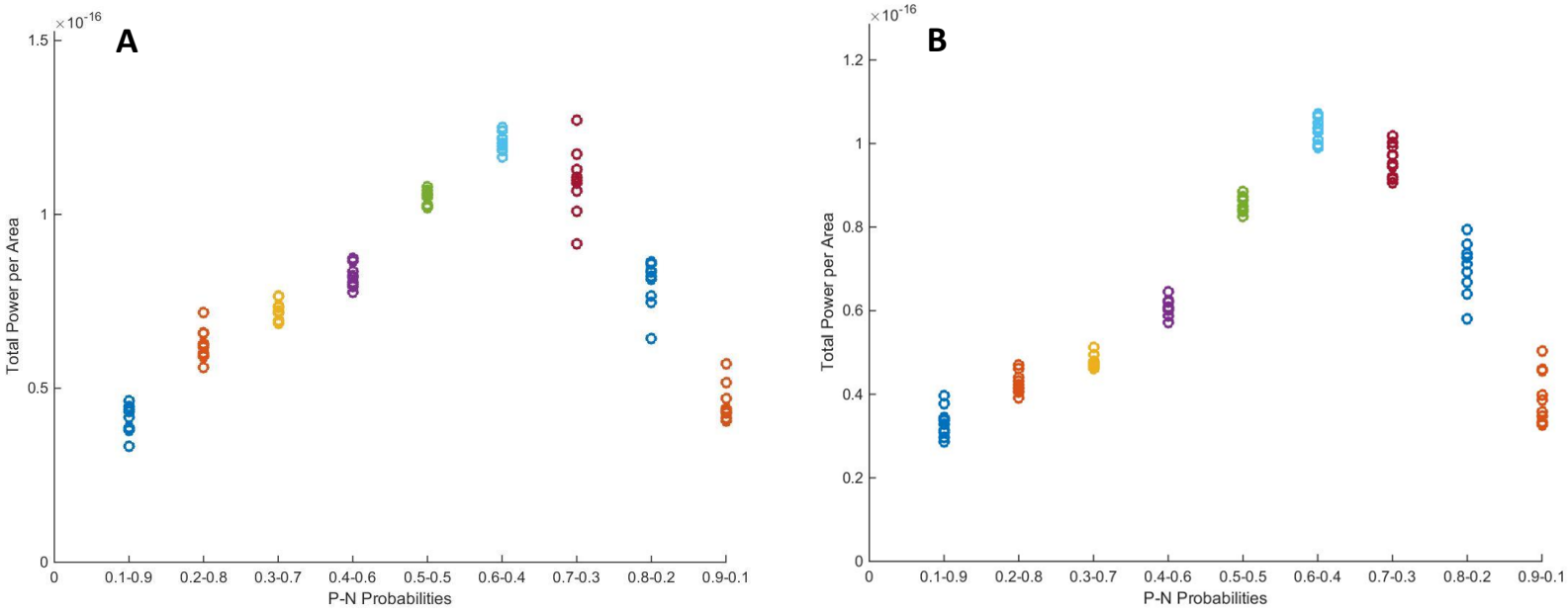

Figure 7. a). Acceptor conductivity σ_2 satisfies $\sigma_2=(0.25*\sigma_1)=2.315 \times 10^{-5}$ $(\Omega*m)^{-1}$. The highest mean power density, at the 60%-40% pair, measures 1.20×10^{-16} W/Area. **b).** The development of a saddle point or local minimum at 30%-70% is more evident. σ_2 is one-eighth the value of σ_1, at 1.1575×10^{-5} $(\Omega*m)^{-1}$. The 60%-40% pair provides the greatest mean power density of 1.03×10^{-16} W/Area.

With $\sigma_2 = \sigma_1 = 9.26 \times 10^{-5}\ (\Omega*m)^{-1}$, the greatest mean power density occurred in the 50%-50% samples (Figure 7c). These results were later used to identify potentially advantageous "capped" samples, as described in part C of this section. Furthermore, they provide insight into the ratios and electrical properties of other[16] potentially favorable donor-acceptor materials.

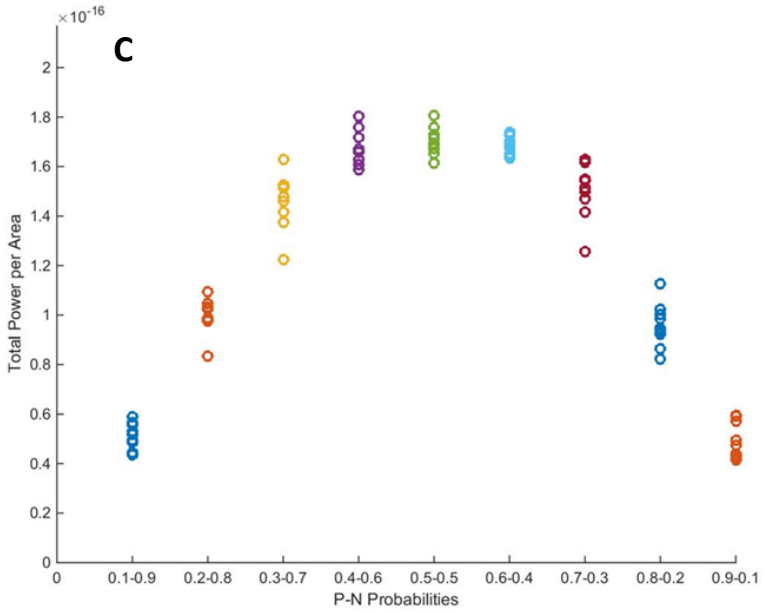

Figure 7 c). Donor-acceptor conductivities satisfied $\sigma_2=\sigma_1=9.26 \times 10^{-5}\ (\Omega*m)^{-1}$. The greatest mean power density, at the 50%-50% probability pair, measures 1.71×10^{-16} W/Area.

B. Gradient Sample

Unlike in part A, the p-n proportions used in these samples varied with the z-coordinates. A unique probability pair $P_1\%$ - $P_2\%$, with $P_2 = 100 - P_1$, was assigned to each of the bulk-heterojunction's 20 layers parallel to the x-y plane. P_1 and P_2 increased and decreased linearly, respectively, with increasing z-coordinates of the specified layers. To ensure convergence using the default $N_{iter} = 8000$, the probabilities were restricted to the range $37.5 \leq P \leq 62.5$. Thirty generated samples produced a mean power density of 9.91×10^{-17}

W/Area and a maximum power density of 1.06 x 10^{-16} W/Area, with standard deviation 3.23 x 10^{-18} W/Area. These results are inferior to the mean power density values obtained in part A. This may be due to the increased likelihood of "islands",[18] pieces of one material completely surrounded by the other material type. Nelson and Schlittenhardt note that such islands promote recombination,[18] trapping charge carriers and reducing usable current reaching the OSC electrodes.[8] A gradient-type sample using the probabilities indicated[19] is therefore not a favorable BHJ to provide high power conversion efficiency.

C. Capped Sample

The third type of sample employed results from the *uniform weighted-sum sample* tests. New BHJ samples were generated to find the optimal implementation of the three favorable probability-pairs 50%-50%, 60%-40% and 70%-30%. The following samples, of height 20 units, consisted of three parts: a bottom and top "cap", each of height 5 units, and a middle portion of height 10 units. These three regions were assigned specific probability pairs before the entire sample was generated in MATLAB. Thirty samples were generated for each morphology. The bulk-heterojunction samples and results are shown in Table 1.

	Sample 1	**Sample 2**	**Sample 3**	**Sample 4**
Data collected after 30 runs (3 trials of 10 runs each)	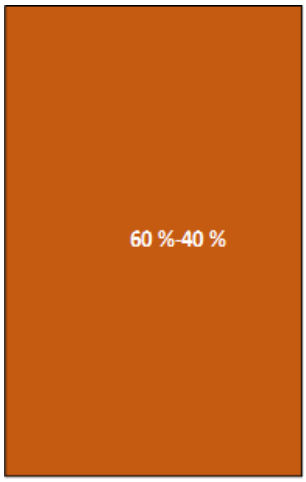	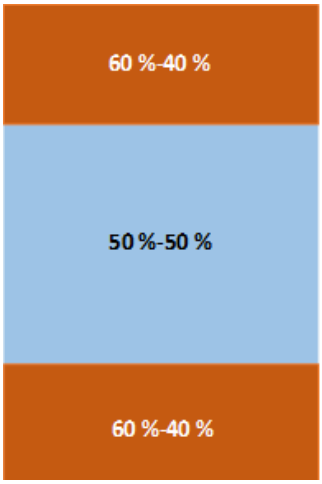	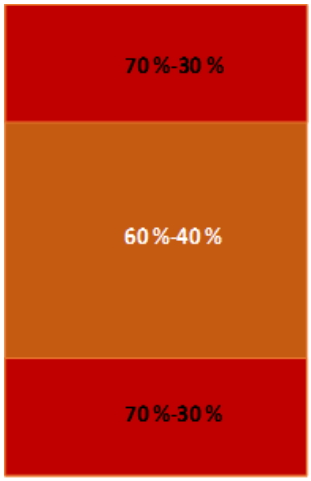	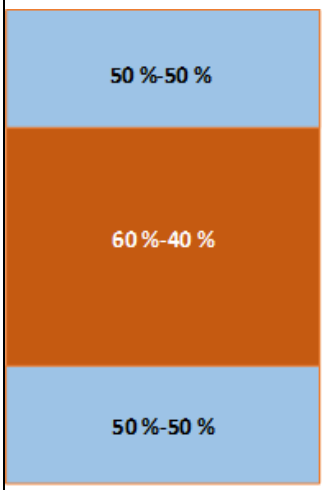
Maximum Net Power Density	1.500e-16 W/Area	1.355e-16 W/Area	1.282e-16 W/Area	1.515e-16 W/Area
Mean Net Power Density	1.435e-16 W/Area	1.248e-16 W/Area	1.173e-16 W/Area	1.442e-16 W/Area
Standard Deviation	4.155e-18 W/Area	3.939e-18 W/Area	6.066e-18 W/Area	4.618e-18 W/Area

Table 1. *Power Density Data from Capped Samples*
Default conductivities σ_1=9.26 x 10^{-5} $(\Omega*m)^{-1}$ and σ_2=4.263 x 10^{-5} $(\Omega*m)^{-1}$ were used in all runs.

Although samples 2 and 4 differ only in the placement of the 50%-50% and 60%-40% regions, their power densities differ significantly. Sample 4 has mean power density 112% that of sample 2, and maximum power density 116% of the value obtained with sample 2. This difference may lie in the use of carrier-specific electrodes, as is necessary in OSCs.[5] The cathode collects electrons, and the anode collects electron holes. For large collection to occur, the cathode must be adjacent to the acceptor material, while the anode must be adjacent to the donor material.[4] When an unequal donor-acceptor probability pair, where $P_1 > P_2$, is used in *both* caps,

the cathode (top electrode) is surrounded by less of its corresponding material (n) and more of the opposite material type (p). This reduces the electric current and net power, as occurs in sample 2. As the cap probabilities become more disparate, as in sample 3, the reduction of current and power is even greater. This disadvantage is avoided in sample 4, where the p-n material ratio near the electrodes approaches 1.

Despite the unequal probability-pair used in sample 1, this BHJ displays mean and maximum power densities nearly equal to those of sample 4. The concept of islands[18] may eliminate this paradox. Due to its single probability-pair characteristic, Sample 1 is less likely to contain islands than the other three samples, providing a large amount of current flow between the electrodes. Samples 1 and 4 are particularly favorable types of bulk-heterojunctions, yet all four samples provide mean and maximum net power densities superior to those of the gradient samples in part B.

V. SUMMARY

The results of this theoretical project reveal various promising bulk-heterojunction morphologies that could increase organic solar cell power conversion efficiency. A sample subjected to the 60%-40% donor-acceptor relationship, as well as a "capped" sample, with probabilities 50%-50%, 60%-40% and 50%-50%, appear to provide examples of favorable bulk-heterojunction forms. The manufacturing feasibility of such BHJ's and the identities of optimal donor/acceptor materials are issues which scientists in other fields must investigate. The future marketability of organic solar cells will require continued cooperation between physicists, chemists and materials scientists in all areas of related research.

ACKNOWLEDGMENTS

I thank Dr. Selman Hershfield and Timothy Schlittenhardt for their guidance and assistance in the course of the 2017 Physics REU Program at the University of Florida. This work was supported by NSF DMR-1461019.

REFERENCES

[1] M. Mayukh, I. H. Jung, F. He and L. Yu, "Incremental optimization in donor polymers for bulk heterojunction organic solar cells exhibiting high performance," *J. Polym. Sci. B Polym. Phys.*, **50**, 1057–1070 (2012).

[2] M. C. Scharber, "On the Efficiency Limit of Conjugated Polymer:Fullerene-Based Bulk Heterojunction Solar Cells," *Adv. Mater.*, **28**, 1994–2001 (2016).

[3] H. Kang, G. Kim, J. Kim, S. Kwon, H. Kim and K. Lee, "Bulk-Heterojunction Organic Solar Cells: Five Core Technologies for Their Commercialization," *Adv. Mater.*, **28**, 7821–7861 (2016).

[4] M.C. Scharber and N.S. Sariciftci, "Efficiency of bulk-heterojunction organic solar cells," *Prog. Polym. Sci.*, **38**, 1929-1940 (2013).

[5] N. Marinova, S. Valero and J.L. Delgado, "Organic and perovskite solar cells: Working principles, materials and interfaces," *J. Colloid Interface Sci.*, **488**, 373-389 (2017).

[6] M. A. Green, K. Emery, Y. Hishikawa, W. Warta, E. D. Dunlop, D. H. Levi and A. W. Y. Ho-Baillie, "Solar cell efficiency tables (version 49)". *Prog. Photovolt: Res. Appl.*, **25**, 3–13 (2017)

[7] M. C. Scharber, D. Mühlbacher, M. Koppe, P. Denk, C. Waldauf, A. J. Heeger and C. J. Brabec, "Design Rules for Donors in Bulk-Heterojunction Solar Cells—Towards 10 % Energy-Conversion Efficiency," *Adv. Mater.*, **18**, 789–794 (2006).

[8] J. Nelson, *The Physics of Solar Cells* (Imperial College, London, 2003), p. 99

[9] I thank Dr. Selman Hershfield for his explanations of this topic.

[10] Another approach is to use the "Model Problem," as presented in David Young's *Iterative Solution of Large Linear Systems* (Academic, New York, 1971), pp 2-6.

[11] D. Young, *Iterative Solution of Large Linear Systems* (Academic, New York, 1971), pp 589-90.

[12] My choice of an appropriate iteration number N_{iter} will be discussed in Section III.

[13] Initial parameters for generation of the OSC bulk-heterojunctions were set by Timothy Schlittenhardt and taken from [17].

[14] I thank Dr. Selman Hershfield and Timothy Schlittenhardt for providing the foundational MATLAB code and important parameters, which were vital components of my own scripts.

[15] T. P. Schlittenhardt, Ph.D. thesis, University of Florida, 2017 (to be published), Sec. 6.1.

[16] Schlittenhardt solely uses the conductivity values $\sigma_1 = 9.26 \times 10^{-5}\ (\Omega*m)^{-1}$ and $\sigma_2 = (0.5*\sigma_1) = 4.63 \times 10^{-5}\ (\Omega*m)^{-1}$.

[17] T. P. Schlittenhardt, Ph.D. thesis, University of Florida, 2017 (to be published), Sec. 2.2.

[18] T. P. Schlittenhardt, Ph.D. thesis, University of Florida, 2017 (to be published), Sec. 4.1.2.

[19] A greater number of iterations ($N_{iter} > 50{,}000$) is needed to test samples in which any probability pair contains a term approaching 5%. For the sake of N_{iter} consistency in this project, such simulations were not performed.